Jamming and unjamming transition of oil-in-water emulsions under continuous temperature change

Se Bin Choi and Joon Sang Lee[a)]
Department of Mechanical Engineering, Yonsei University, 50 Yonsei-ro, Seodaemun-gu, Seoul 120-749, South Korea

(Received 15 March 2015; accepted 28 May 2015; published online 4 June 2015)

To analyze the jamming and unjamming transition of oil-in-water emulsions under continuous temperature change, we simulated an emulsion system whose critical volume fraction was 0.3, which was validated with experimental results under oscillatory shear stress. In addition, we calculated the elastic modulus using the phase lag between strain and stress. Through heating and cooling, the emulsion experienced unjamming and jamming. A phenomenon—which is when the elastic modulus does not reach the expected value at the isothermal system—occurred when the emulsion system was cooled. We determined that this phenomenon was caused by the frequency being faster than the relaxation of the deformed droplets. We justified the relation between the frequency and relaxation by simulating the frequency dependency of the difference between the elastic modulus when cooled and the expected value at the same temperature. © *2015 AIP Publishing LLC*.
[http://dx.doi.org/10.1063/1.4922278]

I. INTRODUCTION

A broad range of rheological materials, such as foams, granular materials, emulsions, and colloidal suspensions, can undergo a transition between a flowing liquid-like (unjammed) state and a nonequilibrium disordered solid (jammed) state. Understanding the mechanism of this transition is of great interest in many research areas in the food, polymer, biomedical, and lubrication industries.[1–3] Especially, the rheological properties of blood as a colloidal suspension have great effects on the blood pressure and wall shear stress related to the cardiovascular diseases. The elastic modulus, determined by the phase lag between strain and stress under oscillatory shear flow, is one factor that can analyze the transition. For liquid, the elastic modulus is zero because the phase lag is 90°. However, the elastic modulus becomes nonzero for a solid-like jammed system because the phase lag is between 0° and 90°, which means that a system deformed by external forces has a tendency to recover its original shape when the forces are removed. Three parameters influence the jammed states: volume fraction, shear stress, and temperature. When increasing the volume fraction, or decreasing the shear stress and temperature, systems tend to go from unjammed to jammed states.[4,5]

The effects of the volume fraction on the jamming or unjamming transition have attracted considerable interest in many studies.[6–20] At the moment, the volume fraction of a system reaches the jamming threshold—the critical volume fraction—the bulk and shear moduli simultaneously become nonzero, and the distribution of the critical volume fraction values becomes narrower as the system size increases.[6] As the volume fraction decreases toward the onset of unjamming, the density of vibrational states approaches a nonzero value in the limit of zero frequency.[7] By continuously and uniformly increasing the packing fraction of a quasi-two-dimensional granular system, a structure signature, which is shown as the maximum of the height of the first peaks of the pair correlation function, was found through the zero-temperature jamming point.[8] Flow curves for the unjammed and jammed states are theoretically described by the

[a)]Author to whom correspondence should be addressed. Electronic mail: joonlee@yonsei.ac.kr

Herschel–Bulkley equation and a cross-type equation, respectively.[9,10] By rescaling the shear stress and shear rate, it is possible to obtain master curves for the flow properties both above and below the jamming with a continuous transition between the two in the shear thinning region.[11] Non-Newtonian behavior below the jamming concentration and yield-stress behavior above it was found.[12]

The dependency of the temperature on the transition has also been studied.[21–23] Scaling of the shear modulus of gel captures the temperature dependence of the shear modulus for different particle sizes and batches entirely within the threshold volume fraction.[21] The temperature becomes independent of the shear rate for a sufficiently slow shear, which suggests that it is an effective temperature for the jammed packing.[22] A maximum in the height of the first peak of the pair-correlation function shifts to higher packing fractions as the temperature is increased from zero.[23] There have been many experimental and numerical studies explaining trends of rheological properties in different isothermal systems.[24–26] However, it is not clear how the transition occurs when the temperature continuously increases or decreases. This lack of clarity exists despite the fact that temperature change is the condition that emulsions may commonly experience in industrial settings. Emulsions can show a different rheological behavior in a continuous temperature change because the temperature effects on the droplets can accumulate in the system.

In this study, we numerically evaluated the feature of a jamming or unjamming transition of an oil-in-water emulsion when the system is cooled or heated. The elastic modulus under the oscillating shear stress was calculated to analyze the transition. The temperature was cooled or heated by constant wall temperature. To validate the developed model, the volume fraction and temperature dependency were compared with the experimental data. The simulation results well corresponded with the experiments. When the emulsion was heated from a specific temperature, that causes the system to jam, to the unjamming temperature, the droplets in the emulsion underwent high deformation, which resulted in well de-aggregation and a low elastic modulus. Therefore, the jammed emulsion became unjammed by heating. In contrast, when the emulsion was cooled from a specific temperature, that caused the system to unjam, to the jamming temperature, the highly deformed droplets from the high temperature could not recover their original shape at low temperature on account of a faster oscillatory frequency than the relaxation of the droplets. As a result, the elastic modulus of the cooled system did not reach that of the isothermal system. Therefore, the unjammed emulsion was frequency-dependently jammed by cooling; moreover, the probability that the jamming transition would occur became higher when the frequency was lower. Through this study, it is possible to analyze the microfluidic rheology without experiments which cause the unexpected jamming at low flow rate and low temperature.[19] All simulations were performed by the 3D lattice Boltzmann method (LBM). The basic jamming/unjamming concept and overall contents and objectives of this paper are outlined in Fig. 1.

II. SIMULATION MODELS

A. 3D thermal lattice Boltzmann model

LBM was developed to analyze the emulsion rheology. The Boltzmann kinetic equation is defined as

$$\frac{\partial f}{\partial t} + c \cdot \nabla f = \Omega(f), \tag{1}$$

where f is the density distribution function, c is the lattice velocity, and $\Omega(f)$ is the collision term. In LBM, the collision term must be simplified by Bhatnagar–Gross–Krook (BGK) approximation on account of its complexity. The simplified equation is then discretized in nineteen specific directions for the D3Q19 model as follows (Fig. 2):

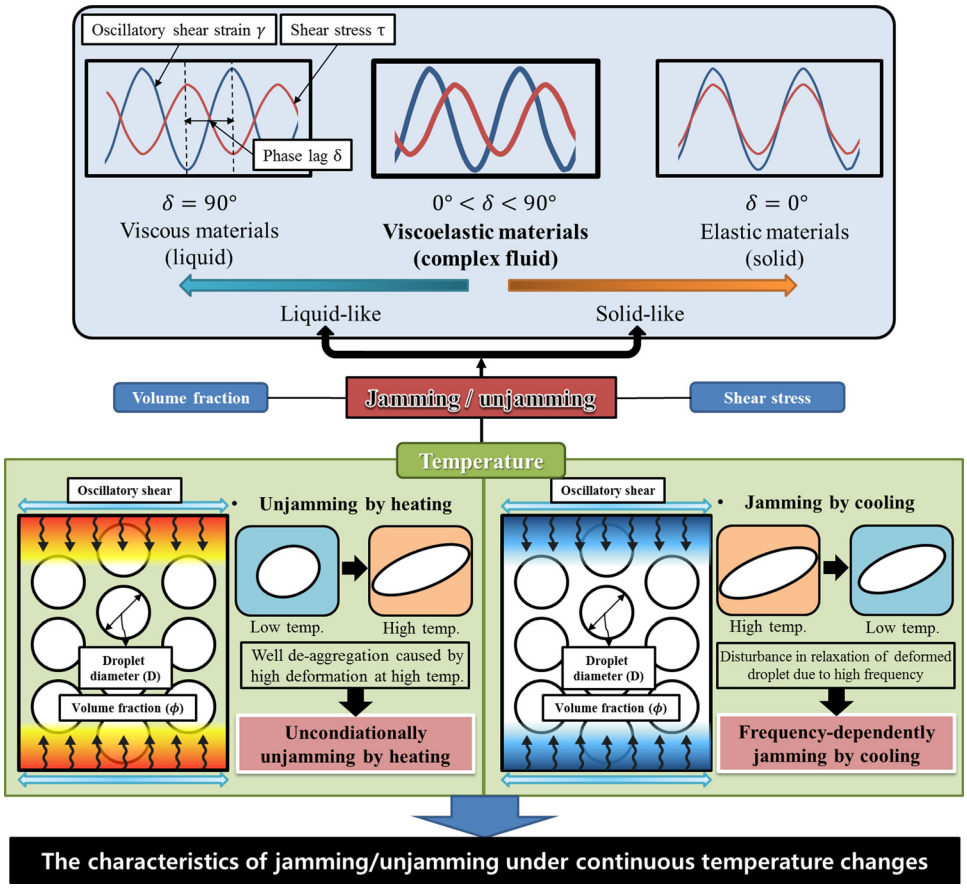

FIG. 1. Schematic diagram summarizing the objectives of the study.

$$f_i(x + c_i\Delta t,\, t + \Delta t) - f_i(x,t) = \frac{\Delta t}{\tau}\left[f_i^{eq}(x,t) - f_i(r,t)\right], \tag{2}$$

where f_{eq} is the equilibrium distribution function, which can be obtained by the following formula:

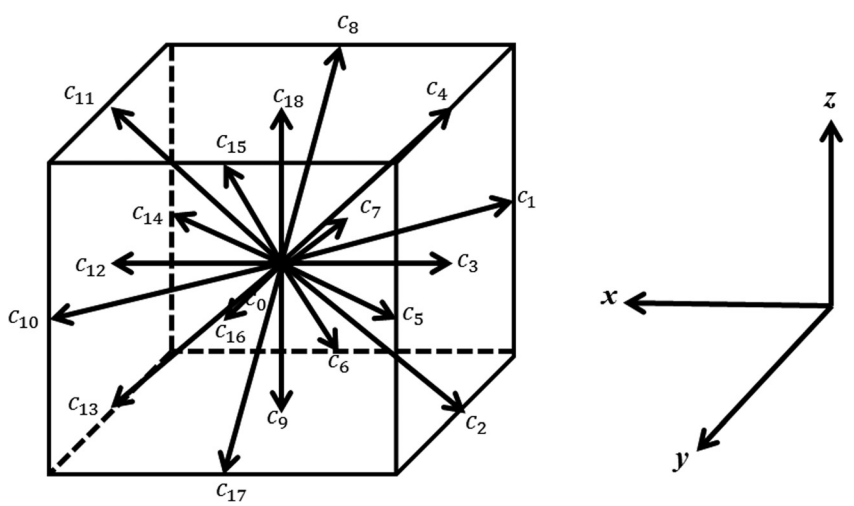

FIG. 2. Lattice links for the D3Q19 lattice Boltzmann method used in this work.

$$f_{eq} = \rho\omega_i\left[1 + \frac{3}{c^2}c_i \cdot \boldsymbol{u} + \frac{9}{2c^4}(c_i \cdot \boldsymbol{u})^2 - \frac{3}{2c^2}\boldsymbol{u} \cdot \boldsymbol{u}\right], \tag{3}$$

where ω_i is the weighting factor that determines the relative probability of a particle movement in the ith direction, and ρ and $\boldsymbol{u}$ are the macroscopic density and velocity, which are calculated as follows:

$$\rho = \sum_{i=0}^{Q-1} f_i = \sum_{i=0}^{Q-1} f_i^{eq}, \tag{4}$$

$$\rho \mathrm{u} = \sum_{i=0}^{Q-1} c_i f_i = \sum_{i=0}^{Q-1} c_i f_i^{eq}. \tag{5}$$

Relaxation time τ of Eq. (2) is related to the kinematic viscosity as follows:

$$\nu = (\tau - 0.5)\mathrm{c}_\mathrm{s}^2 \Delta t, \tag{6}$$

where $\mathrm{c_s}$ is the lattice speed of sound, and lattice time step Δt is taken as unity. For isothermal flow, the relaxation time is fixed throughout the entire simulation time. However, if the viscosity is changed by temperature, the relaxation time should be locally changed accordingly. In this paper, τ changes according to the local temperature change

$$\frac{\tau(T) - 0.5}{\tau_0 - 0.5} = \frac{\mu(T)}{\mu_0} = \left(\frac{T}{T_0}\right)^{-1.0868}. \tag{7}$$

Gunstensen and Rothman[27] simulated a two-immiscible fluid emulsion using LBM. The total distribution function is expressed by the summation of the two red-and-blue fluid distribution functions as follows:

$$f_i = r_i + b_i. \tag{8}$$

To create a phase field, the interfacial density between two fluids is defined

$$\rho^N = \frac{r_i - b_i}{r_i + b_i}. \tag{9}$$

Lishchuk *et al.*[28] employed the following macroscopic force (F(x)) to apply the interfacial tension force:

$$F(x) = -\frac{1}{2}\alpha k \nabla \rho^N, \tag{10}$$

where α is the interfacial tension and k is the droplet curvature. The relationship between the source term in the LBM equation and macroscopic force F(x) is calculated by the method of Guo *et al.*,[29]

$$\phi_\mathrm{i}(x) = \omega_i\left(1 - \frac{1}{2\tau}\right)\left[3(\mathrm{e_i} - u^*) + 9(e_i u^*)e_j\right]F(x), \tag{11}$$

$$\mathrm{u}^* = \frac{1}{\rho}\left[\sum_{i=1}^{18} f_i e_i + \frac{1}{2}F(x)\right], \tag{12}$$

where u^* is the corrected velocity used in the calculation of the equilibrium function. The local interfacial tension affects the surface tension force, which subsequently influences the corrected

velocity. From that point, the fluid is separated into two parts, red and blue fluids, using the following relationship:

$$\bar{\bar{f}}_i^{\mathrm{R}}(x,\, t+\delta_t) = \frac{\rho^{\mathrm{R}}}{\rho^{\mathrm{R}}+\rho^{B}}\bar{f}_i(x,\, t+\delta_t) + \beta\frac{\rho^{R}\rho^{B}}{\rho^{\mathrm{R}}+\rho^{\mathrm{B}}}\omega_i\cos\left(\theta_f-\theta_i\right)|c_i|, \tag{13}$$

$$\bar{\bar{f}}_i^{\mathrm{B}}(x,\, t+\delta_t) = \bar{f}_i(x,\, t+\delta_t) - \bar{\bar{f}}_i^{\mathrm{R}}(x,\, t+\delta_t), \tag{14}$$

where $\bar{\bar{f}}_i^{\mathrm{R}}$ and $\bar{\bar{f}}_i^{\mathrm{B}}$, respectively, denote the post-collision and post-segregation distribution functions of the red and blue fluids, and θ_f and θ_i are the polar angle of the color field and the angle of the velocity link, respectively. In addition, the segregation parameter is β, and $\bar{f}_i$ is the post-collision distribution function. After segregation, these two fluids are separately propagated and macroscopic properties are obtained through each distribution function.

Many models have been developed to apply the thermal phenomena in LBM.[30,31] The thermal phenomena of an emulsion system are governed by the following energy equation:

$$\frac{DT}{Dt} + (\nabla\cdot\boldsymbol{u})T - D\nabla^2 T + \Phi = 0, \tag{15}$$

where T is the local temperature, D is the thermal diffusivity, and Φ is the dissipation term, which is expressed as follows:

$$\Phi = \mu(\mathrm{T})\left\{\begin{array}{l} 2\left[\left(\frac{\partial u_x}{\partial x}\right)^2+\left(\frac{\partial u_y}{\partial y}\right)^2+\left(\frac{\partial u_z}{\partial z}\right)^2\right]+\left(\frac{\partial u_x}{\partial y}+\frac{\partial u_y}{\partial x}\right)^2 \\ \quad +\left(\frac{\partial u_x}{\partial z}+\frac{\partial u_z}{\partial x}\right)^2+\left(\frac{\partial u_y}{\partial z}+\frac{\partial u_z}{\partial y}\right)^2 \end{array}\right\} - \frac{2}{3}\mu(T)(\nabla\cdot\boldsymbol{u})^2, \tag{16}$$

where $\mu(T)$ is the temperature-dependent viscosity, and u_x, u_y, and u_z are the velocity components of x, y, and z directions, respectively. The hopscotch explicit and unconditionally stable finite difference methods were used here to solve the energy equation. This scheme uses two consecutive sweeps through the domain. The first sweep, $\mathrm{T}_{i,j}^{n+1}$, is calculated at each grid, for which $i+j+n$ is even, by a simple explicit scheme. The second sweep, $\mathrm{T}_{i,j}^{n+1}$, is calculated at each grid point, for which $i+j+n$ is odd, by a simple implicit scheme.

B. Surfactant model

The surfactant transport on the droplet interface is governed by the following time-dependent convective-diffusion equation:[32]

$$\frac{\partial\Gamma}{\partial t} + \nabla_s\cdot(u_s\Gamma) + k\Gamma u_n = D_s\nabla^2\Gamma, \tag{17}$$

where Γ is the surfactant concentration, u_s, u_n are the surface velocity and normal velocity, k is the surface curvature, and D_s is the surfactant diffusivity, both of which were calculated from the MD simulation. In Eq. (17), $\partial_t\Gamma$ signifies the change in the local surfactant concentration as time flows, $\nabla_s\cdot(u_s\Gamma)$ is the convection term relating to interfacial velocity, and $k\Gamma u_n$ shows how surface curvature affects the surfactant concentration. The right term, $D_s\nabla^2\Gamma$, is the diffusive contribution. As with solving the energy equation, the hopscotch explicit finite difference method is used to solve the convective-diffusion equation and is then coupled with Gunstensen LBM. More information on the solution of the convective-diffusion equation can be found in previous work.[33]

C. Oscillatory shear stress

The top and bottom walls of the simulation domain oscillate according to the following:

$$u_w(\omega, t) = \frac{H}{2}\gamma_0 \omega \cos \omega t, \tag{18}$$

where H is the height, γ_0 is the strain amplitude of the oscillation, and ω is the frequency. This velocity profile was applied on LBM as the Dirichlet boundary condition. The stress caused by the velocity condition was delayed with phase lag δ, which was above 0° and below 90°, because the emulsion was viscoelastic. Therefore, the shear stress can be expressed and calculated by the following formula:

$$\tau = \tau_0 \sin(\omega t + \delta) = \mu_{eff} \frac{\partial u_x}{\partial z}, \tag{19}$$

where μ_{eff} is the effective viscosity of the emulsion. From phase lag δ, the elastic modulus can be computed as follows:

$$G' = \frac{\tau_0}{\gamma_0} \cos \delta. \tag{20}$$

In this study, the elastic modulus values were averaged in one period of the oscillation.

III. RESULTS

A. Model validation

To validate the present model, the critical volume fraction, the strain amplitude-dependent, and the temperature-dependent elastic modulus were simulated and compared with the experimental data.[34,35] In the experiment,[34] an emulsion composed of paraffin-oil droplets in water were used along with three volume fractions (0.1, 0.2, and 0.3). In our simulations, the number of droplets was used to control the volume fraction. Figure 3 shows the initial and middle state of the simulation domain for each volume fraction. The average diameter of droplets was 2 μm, the frequency was fixed to 6.28/s, and the temperature was 25 °C for all volume fractions.

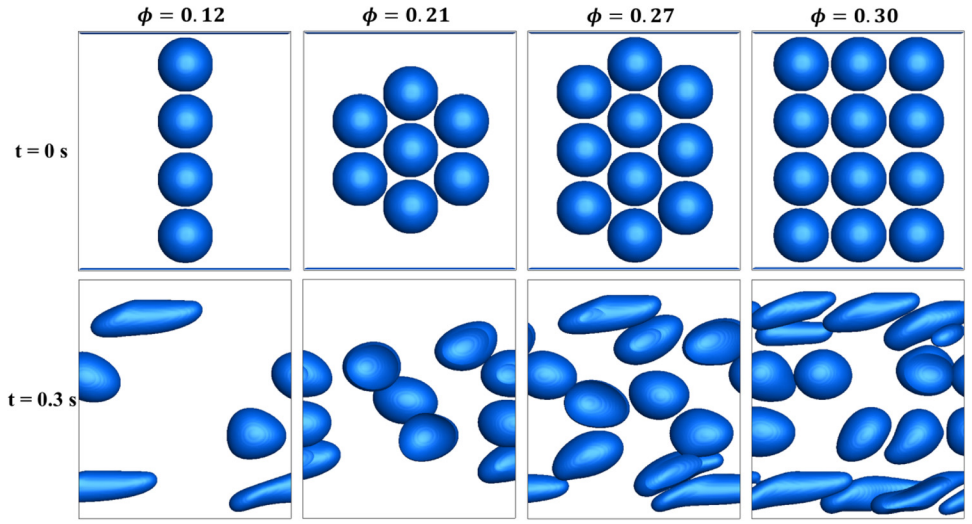

FIG. 3. The number of droplets was used to control the volume fraction of emulsion. As time evolved, the droplets were mixed by the oscillating shear flow, but never combined together due to the suppression of coalescence.

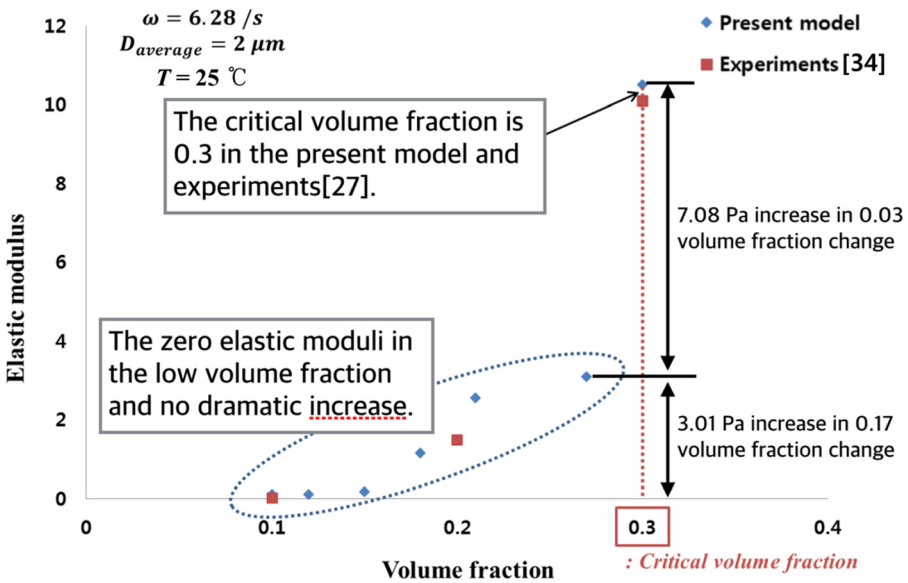

FIG. 4. Jamming transition at ϕ in both the proposed model and the experiments.

As shown in Fig. 4, the elastic modulus had very small values when the volume fraction was less than 0.2. However, the value of the elastic modulus jumped to 10.1 Pa at the volume fraction $\phi = 0.3$, which means that critical volume fraction ϕ_c was approximately 0.3. This trend corresponded well with the experimental results, as shown in Fig. 4. Although the absolute values of our simulation results were slightly higher than those of the experimental results, the elastic modulus significantly increased at $\phi_c \approx 0.3$. Through these results, the jamming transition with an increase in volume fraction could be observed in the proposed model. Figure 5 shows the elastic modulus as a function of the strain amplitude. At the certain strain amplitude ($\gamma_0 \approx 2$), the elastic modulus began to decrease as the strain increased both in the present model and the experiment, which means that the emulsion has the yield stress at $\gamma_0 \approx 2$.

To evaluate the suitability of the model with a function of temperature, we validated the proposed model with the experimental results, as shown in Fig. 6. Although Chen and Dickinson,[35] which we referenced for the validation, did not analyze the jamming or

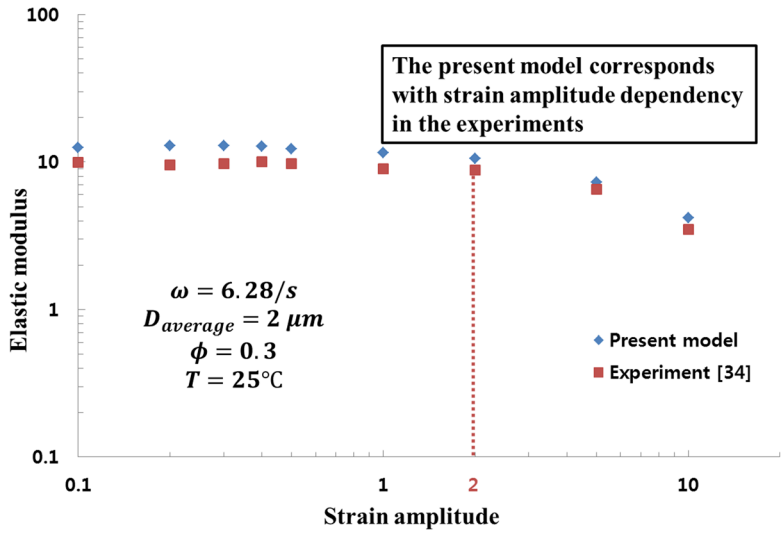

FIG. 5. Strain amplitude dependency on the elastic modulus in the proposed model and the experiments.

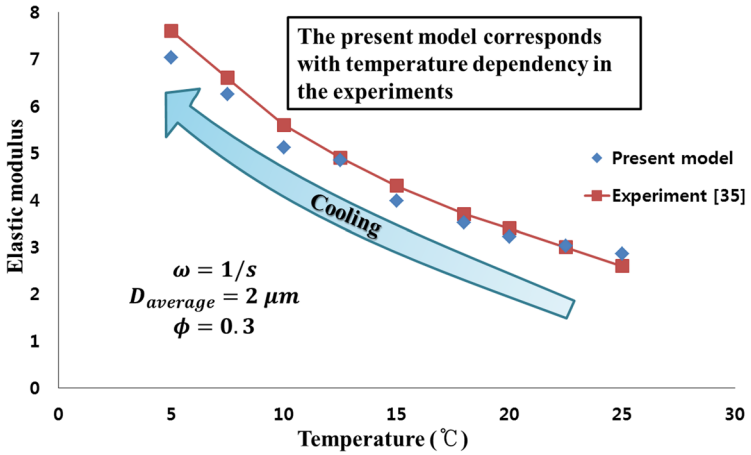

FIG. 6. Temperature dependency on the elastic modulus in the proposed model and the experiments.

unjamming transition, they determined the effects of the prescribed temperature of an emulsion gel on the temperature reversibility of the viscoelasticity. We selected the case showing the reversibility of the elastic modulus to validate the temperature-dependent elastic modulus. In that case, the frequency and volume fraction were 1/s and 0.3, respectively. Oil droplets were 2 μm in diameter, and water as a continuous phase was used. The emulsion system was heated from 25 °C to 45 °C and then cooled to 5 °C. In these series, the elastic modulus was calculated and showed the temperature reversibility. The simulation results in Fig. 5 well corresponded with the experimental results, which shows that the elastic modulus decreased as the temperature increased.

B. Heating from jammed systems

Figure 7 shows the simulation domain and boundary conditions for the heating cases. The droplet diameter and initial strain were fixed to 2 μm and 1, respectively. The top and bottom walls reversely oscillated with frequency ω; moreover, the emulsion was heated or cooled through walls until the average system temperature became the constant wall temperature.

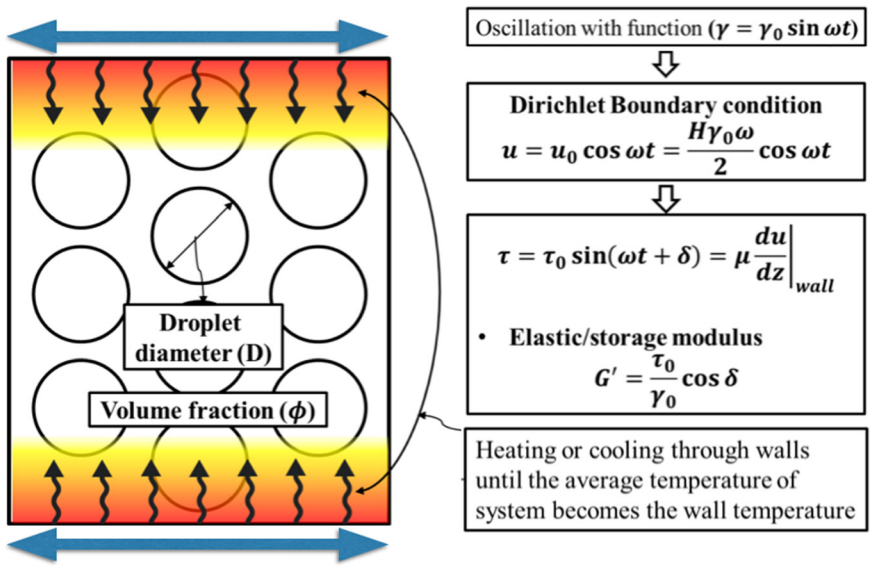

FIG. 7. Simulation domain and boundary conditions.

The viscosities of water and oil were 1 cP and 1000 cP at $T = 20\,^{\circ}C$ and followed Eq. (7) as the temperature changed. The heat capacities of water and oil were 4.18 J/g K and 2.13 J/g K, and the thermal diffusivity of water and oil was 0.143 mm^2/s and 0.081 mm^2/s, respectively. The elastic modulus was calculated by the phase lag between the strain and stress, as mentioned in Sec. II C.

When an emulsion system is heated, the shear modulus typically decreases, and the system behaves more like liquid than solid.[36,37] Therefore, an unjamming transition can be found when a jammed system is heated. At a relatively low temperature, this unjamming transition suddenly occurs, whereas at a relatively high temperature, the transition gradually occurs because the shear modulus is more sensitive at low temperatures.[26] To analyze this phenomenon, the jammed emulsion system (volume fraction $\phi = 0.27$) was heated from 5 °C to 25 °C. The result was compared with isothermal cases (25 °C).

As shown in Figs. 8(a) and 8(b), the characteristics of the elastic modulus changed in the heated systems were different from those in the isothermal systems. In the isothermal systems, the emulsion reached the critical value in the elastic modulus at temperature $T = 7.5\,^{\circ}C$, while the elastic modulus continuously decreased when the system was heated. In the isothermal system, the maximum deformation does not change with time. Therefore, the emulsion is jammed at the critical temperature. In the heated system, the maximum deformation changes as time evolution due to the temperature change. In addition, each droplet has the different maximum deformation because of the temperature gradient. Therefore, the elastic modulus decreases continuously even though the emulsion is partially jammed. However, there was no significant difference between the values of the elastic modulus in the respective heated and isothermal systems at $T = 25\,^{\circ}C$. At low temperature, the resistance force against oscillatory shear stress was strong, and the droplets in the emulsion slightly deformed. As the temperature increased, the droplets adapted well to the shear stress because of the low surface tension and viscosity, which results in greater deformation and a lower elastic modulus. Finally, the elastic modulus reached the value obtained by the isothermal (25 °C) simulation when the average temperature of the emulsion became 25 °C. In Conclusion, the unjamming transition gradually proceeded when the emulsion system was heated, while the unjamming transition suddenly occurred below the critical temperature in the isothermal system.

C. Cooling from unjammed systems

Unlike in Sec. III B, a jamming transition can occur when an unjammed system is cooled. To analyze how this jamming transition occurs, we simulated the cases in which the system unjammed at 25 °C and jammed at 5 °C and was cooled from 25 °C to 5 °C. The volume fraction was 0.27. The results were compared with the isothermal cases (5 °C). The average temperature of the simulation domain decreased with the cooling rate = 19.53 °C/s and diverged to the wall temperature (Fig. 9(a)). As shown in Fig. 9(b), there existed the temperature gradient during the cooling process and the temperature of the whole domain was close to wall temperature at the steady state.

As shown in Fig. 10, the elastic modulus at the steady state did not reach the value obtained at constant temperature (5 °C). The remarkable difference between the values of the elastic modulus in the cooled system and in the isothermal system can be explained by the relaxation of the deformed droplets. The droplets that were highly deformed at higher temperature were no longer deformed as the temperature decreased on account of higher surface tension and viscosity. Then, the deformed droplets tended to recover their original shape and sphere; accordingly, the elastic modulus increased. However, if the frequency of the oscillatory shear was faster than the relaxation of the deformed droplets, the droplets retained their deformation and de-aggregation. Therefore, the elastic modulus in our simulations did not increase and became lower than the isothermal case.

To justify that the relation between the frequency of the oscillatory shear and relaxation of the droplets is a key factor in determining the elastic modulus at the steady state of the cooled system, we obtained the frequency dependency of the elastic modulus. Figure 11(a) shows that

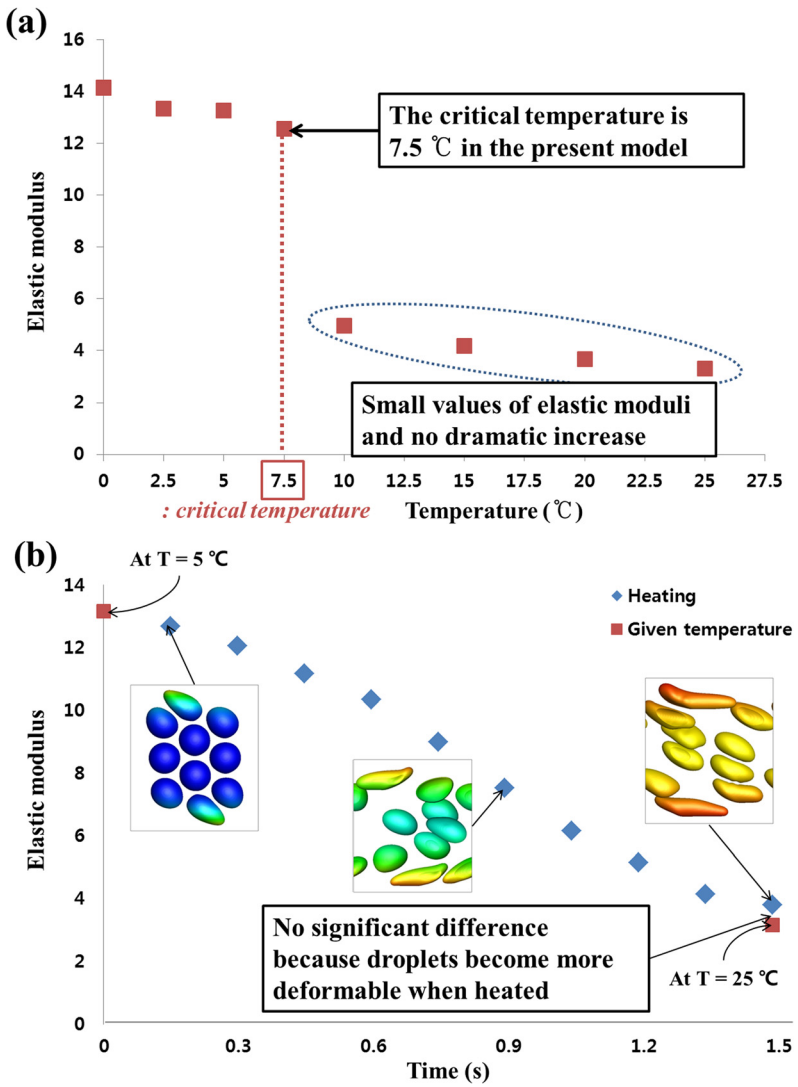

FIG. 8. (a) Emulsion in the proposed model at the critical temperature of 7.5 °C. (b) Elastic modulus as the jammed emulsion is heated, and temperature contour at three time steps (0.3 s; 0.9 s; and 1.5 s).

the difference between the values of the elastic modulus in the cooled system and isothermal system increased with an increase in frequency. This means that the deformed droplets could more easily recover their original shape when the emulsion was cooled in low frequency, which resulted in higher elastic moduli. Even if the frequency is low enough, there is the difference between the elastic modulus in the cooled and isothermal system because the oscillation shear interrupt the droplets to recover their original shape. This phenomenon can be proved by plotting the deformation rate for each frequency. As shown in Fig. 11(b), the average deformation of the droplets at the steady state increased with an increase in frequency for cooling systems. This indicates that, at the steady state, the droplets tended to conform better through external forces at the higher frequency for cooling systems. The average distance between droplets increases with increasing applied shear frequency (see Fig. 11(c)), meaning that droplets interacted less often at higher frequencies. The frequent interactions between droplets resulted in high elastic modulus. In order to investigate how the droplets align with the shear direction, a deformation angle was measured in Fig. 11(d). The deformation angle increased with an increase in frequency, which indicates that the droplets in the emulsion system well adapted to the shear stress. In Conclusions, when the emulsion is cooled at higher frequency, the elastic

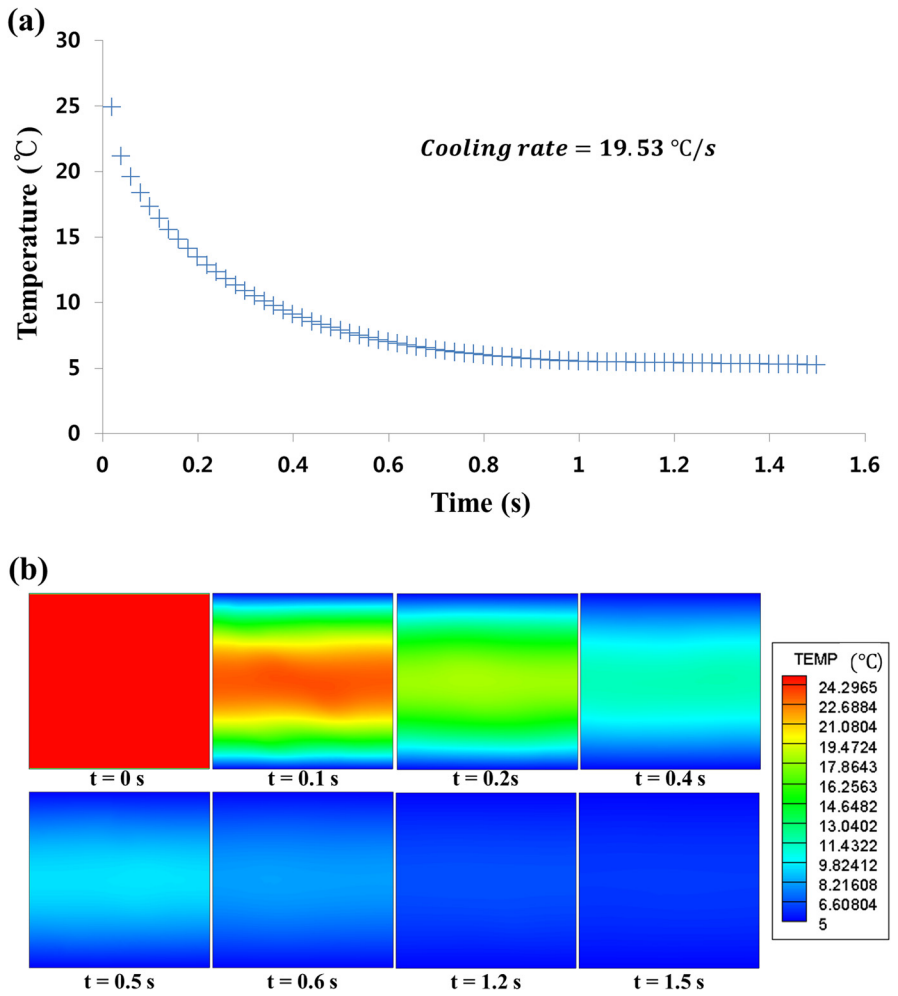

FIG. 9. (a) Average temperature decreases as time evolution with the cooling rate = 19.53 °C/s. (b) The change of the temperature gradient of the domain as time evolution.

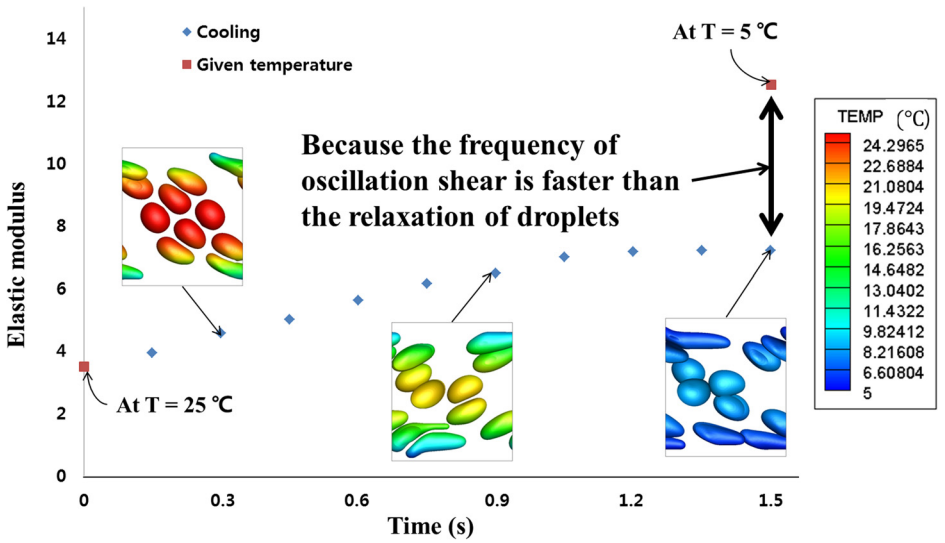

FIG. 10. Elastic modulus as the unjammed emulsion is cooled, and temperature contour at three time steps (0.3 s; 0.9 s; and 1.5 s).

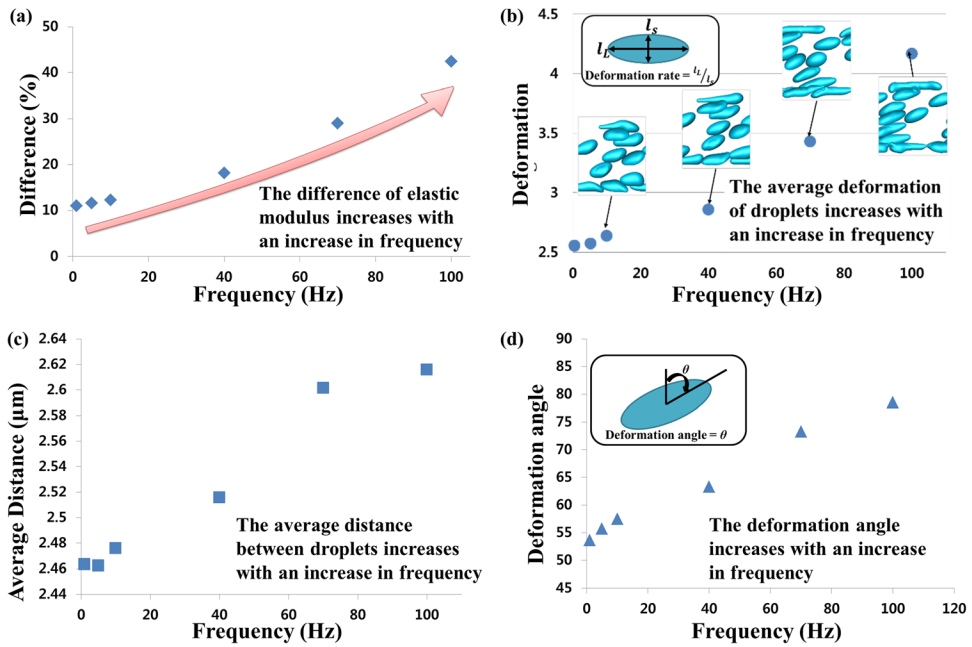

FIG. 11. (a) Frequency dependency on the difference between the values of the elastic modulus in respective cooled and isothermal systems. (b) Average deformation of droplets in emulsion at different frequency values. (c) Average distance between droplets in emulsion at different frequency values. (d) Deformation angle of droplets at different frequency values.

moduli cannot reach those at the jammed state in the isothermal system, which indicates that the emulsion is not jammed for higher frequency in the cooling system.

IV. CONCLUSIONS

Jamming and unjamming transitions of emulsion systems caused by cooling and heating were observed, and the phenomena mechanism was analyzed in terms of the geometric features of the droplets in the emulsions. The proposed model was validated with the experimental results with respect to the critical volume fraction and temperature-dependent elastic modulus; the simulations and experiments well corresponded. The jammed system at 5 °C was heated to 25 °C, and the unjamming transition was observed. In our model, when the unjamming transition occurred, the elastic modulus gradually decreased and reached the value for the isothermal (25 °C) system. On the other hand, if the unjammed system at 25 °C was cooled to 5 °C, the elastic modulus gradually increased and did not reach the value for the isothermal (5 °C) system during the jamming transition. This was because the frequency of oscillation was faster than the relaxation of the deformed droplets. As the frequency decreased, the difference between the elastic modulus of cooled and isothermal cases decreased, which means that there is a close relation between the frequency and relaxation of the droplets.

ACKNOWLEDGMENTS

This work was supported by a Grant from the Mid-career Researcher Program of the National Research Foundation of Korea (NRF) funded by the Ministry of Science, ICT and Future Planning (Grant No. NRF-2013R1A2A2A01015333).

[1]G. Biroli, Nat. Phys. **3**, 222 (2007).
[2]D. Bi, J. Zhang, B. Chakraborty, and R. P. Behringer, Nature **480**, 355 (2011).
[3]H. S. Park and T. T. Nguyen, J. Comput. Des. Eng. **1**, 256 (2014).
[4]M. E. Cates, J. P. Wittmer, J. P. Bouchaud, and P. Claudin, Phys. Rev. Lett. **81**, 1841 (1998).
[5]A. J. Liu and S. R. Nagel, Nature **396**, 21 (1998).
[6]V. Trappe, V. Prasad, L. Cipelletti, P. N. Segre, and D. A. Weitz, Nature **411**, 772 (2001).
[7]C. S. O'Hern, L. E. Silbert, A. J. Liu, and S. R. Nagel, Phys. Rev. E **68**, 011306 (2003).

[8]L. E. Silbert, A. J. Liu, and S. R. Nagel, Phys. Rev. Lett. **95**, 098301 (2005).
[9]X. Cheng, Phys. Rev. E **81**, 031301 (2010).
[10]C. Macosko, *Rheology: Principles, Measurements, and Applications* (Wiley, 1994).
[11]J. Mewis and N. Wagner, *Colloidal Suspension Rheology* (Cambridge University Press, 2012).
[12]K. N. Nordstrom, E. Verneuil, P. E. Arratia, A. Basu, Z. Zhang, A. G. Yodh, J. P. Gollub, and D. J. Durian, Phys. Rev. Lett. **105**, 175701 (2011).
[13]A. Ikeda, L. Berthier, and G. Biroli, J. Chem. Phys. **138**, 12A507 (2013).
[14]C. Reichhardt and C. J. Olson Reichhardt, Soft Matter **10**, 2932 (2014).
[15]J. Brujić, C. Song, P. Wang, C. Briscoe, G. Marty, and H. A. Makse, Phys. Rev. Lett. **98**, 248001 (2007).
[16]J. Brujić, P. Wang, C. Song, D. L. Johnson, O. Sindt, and H. A. Makse, Phys. Rev. Lett. **95**, 128001 (2005).
[17]Y. Jin and H. A. Makse, Physica A **389**, 5362 (2010).
[18]C. Briscoe, C. Song, P. Wang, and H. A. Makse, Phys. Rev. Lett. **101**, 188001 (2008).
[19]H. A. Makse, J. Brujić, and S. F. Edwards, "Statistical mechanics of jammed matter," in *The Physics of Granular Media* (Wiley-VCH, Weinheim, 2004).
[20]A. Basu, Y. Xu, T. Still, P. E. Arratia, Z. Zhang, K. N. Nordstrom, J. M. Rieser, J. P. Gollub, D. J. Durian, and A. G. Yodh, Soft Matter **10**, 3027 (2014).
[21]M. C. Grant and W. B. Russel, Phys. Rev. E **47**, 2606 (1993).
[22]F. Q. Potiguar and H. A. Makse, Eur. Phys. J. E **19**, 171 (2006).
[23]L. E. Silbert, A. J. Liu, and S. R. Nagel, Phys. Rev. E **73**, 041304 (2006).
[24]M. L. Ferrer, C. L. Lawrence, B. G. Demirjian, D. Kivelson, C. Alba-Simionesco, and G. Tarjus, J. Chem. Phys. **109**, 8010 (1998).
[25]T. Nagatani, Phys. Rev. E **58**, 4271 (1998).
[26]Z. Zhang, N. Xu, D. T. N. Chen, P. Yunker, A. M. Alsayed, K. B. Aptowicz, P. Habdas, A. J. Liu, S. R. Nagel, and A. G. Yodh, Nature **459**, 230 (2009).
[27]A. K. Gunstensen and D. H. Rothman, Phys. Rev. A **43**, 4320 (1991).
[28]S. Lishchuk, C. Care, and I. Halliday, Phys. Rev. E **67**, 036701 (2003).
[29]Z. Guo, C. Sheng, and B. Shi, Phys. Rev. E **65**, 046308 (2002).
[30]X. He, S. Chen, and G. D. Doolen, J. Comput. Phys. **146**, 282 (1998).
[31]Z. Guo and T. S. Zhao, Prog. Comput. Fluid Dyn. **5**, 110 (2005).
[32]H. A. Stone, Phys. Fluids A **2**, 111 (1990).
[33]H. Farhat, F. Celiker, T. Singh, and J. S. Lee, Soft Matter **7**, 1968 (2011).
[34]R. Shu, W. Sun, T. Wang, C. Wang, X. Liu, and Z. Tong, Colloids Surf., A **434**, 220 (2013).
[35]J. Chen and E. Dickinson, Int. Dairy J. **10**, 541 (2000).
[36]L. Berthier and J. Barrat, Phys. Rev. Lett. **89**, 095702 (2002).
[37]A. J. Liu and S. R. Nagel, Annu. Rev. Condens. Matter Phys. **1**, 347 (2010).